Science Advances
AAAS

advances.sciencemag.org/cgi/content/full/5/9/eaaw0759/DC1

# Supplementary Materials for

## Initial soil microbiome composition and functioning predetermine future plant health

Zhong Wei, Yian Gu, Ville-Petri Friman, George A. Kowalchuk, Yangchun Xu*, Qirong Shen*, Alexandre Jousset

*Corresponding author. Email: shenqirong@njau.edu.cn (Q.S.); ycxu@njau.edu.cn (Y.X.)

Published 25 September 2019, *Sci. Adv.* **5**, eaaw0759 (2019)
DOI: 10.1126/sciadv.aaw0759

**The PDF file includes:**

**Other Supplementary Material for this manuscript includes the following:**

(available at advances.sciencemag.org/cgi/content/full/5/9/eaaw0759/DC1)

Data file S1 (Microsoft Excel format). Screened OTUs enriched in initial soil microbiome associated with later healthy and diseased plants.
Data file S2 (Microsoft Excel format). Functional genes significantly different in initial soil microbiome associated with later healthy and diseased plants.
Data file S3 (Microsoft Excel format). Screened OTUs enriched in soil microbiome associated with later healthy and diseased plants at 6 week after planting.
Data file S4 (Microsoft Excel format). Functional genes significantly different in soil microbiome associated with later healthy and diseased plants at 6 weeks after planting.
Movie S1 (.mp4 format). Method of sampling middle-layer nylon bags from rhizobox.

## Supplementary materials

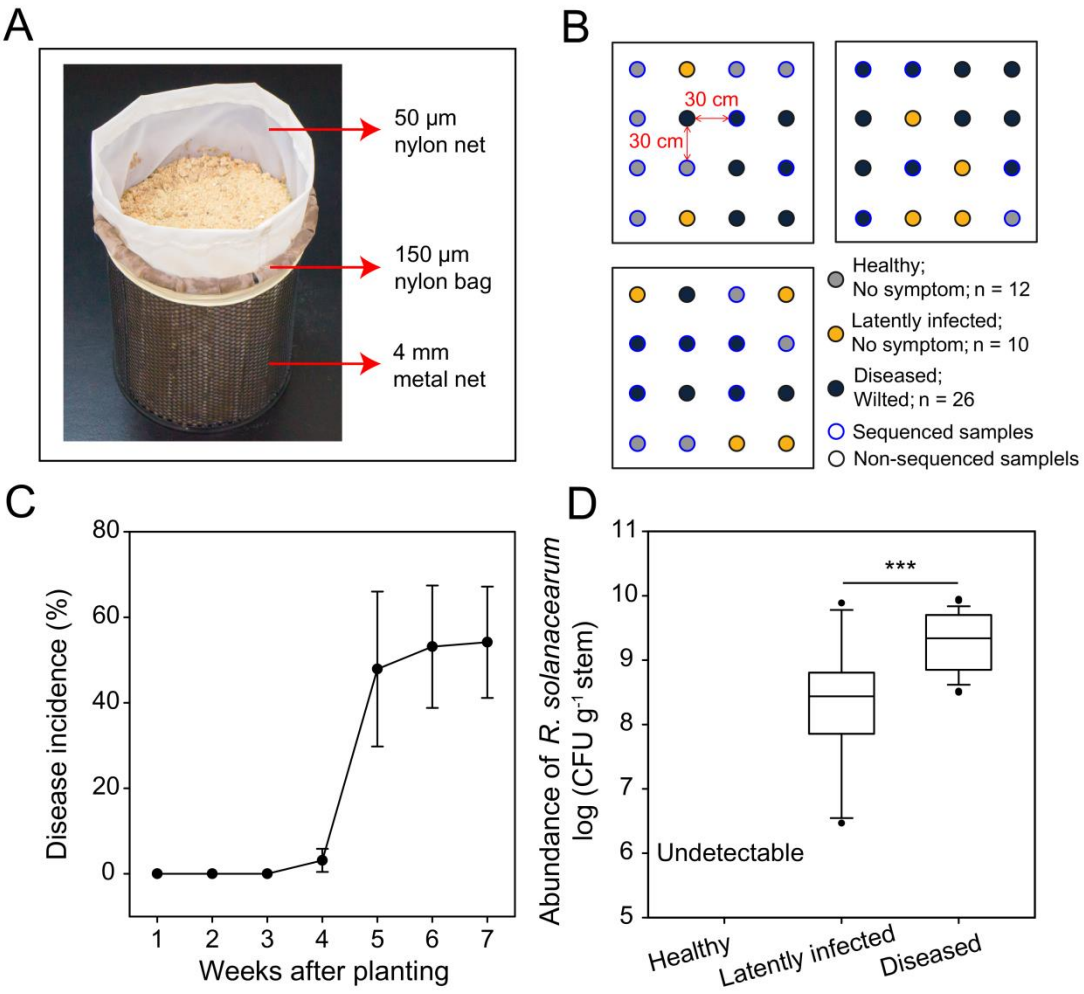


**Fig. S1. The placement of rhizoboxes and observed disease dynamics during the field experiment.** (**A**) Real picture of the rhizobox used in this study (Photo credit: Yian Gu, Nanjing Agricultural University). (**B**) Placement of rhizoboxes (denoted by circle) in replicate plots and different disease outcomes at the end of the field experiment (labeled in different colors). (**C**) The dynamics of bacterial wilt disease incidence during the field experimnt. Disease incidence is represented by the percentage of tomato seedlings with wilt symptoms (Mean ± SD, N = 3 plots with 16 plants each). (**D**) The abundances of *R.*

*solanacearum* pathogen in tomato stem crowns at the end of field experiment (week 7). Pathogen population densities were determined by colony counting and *** indicate significant difference at level $p < 0.001$ (Student's t-test). Plants that showed no wilt symptoms and did not contain detectable *R. solanacearum* in stem crowns were classified as healthy plants. Plants that showed wilt symptoms and contained detectable *R. solanacearum* were classified as diseased plants. Latently infected plants refer to plants that did not show wilt symptoms but contained detectable *R. solanacearum*.

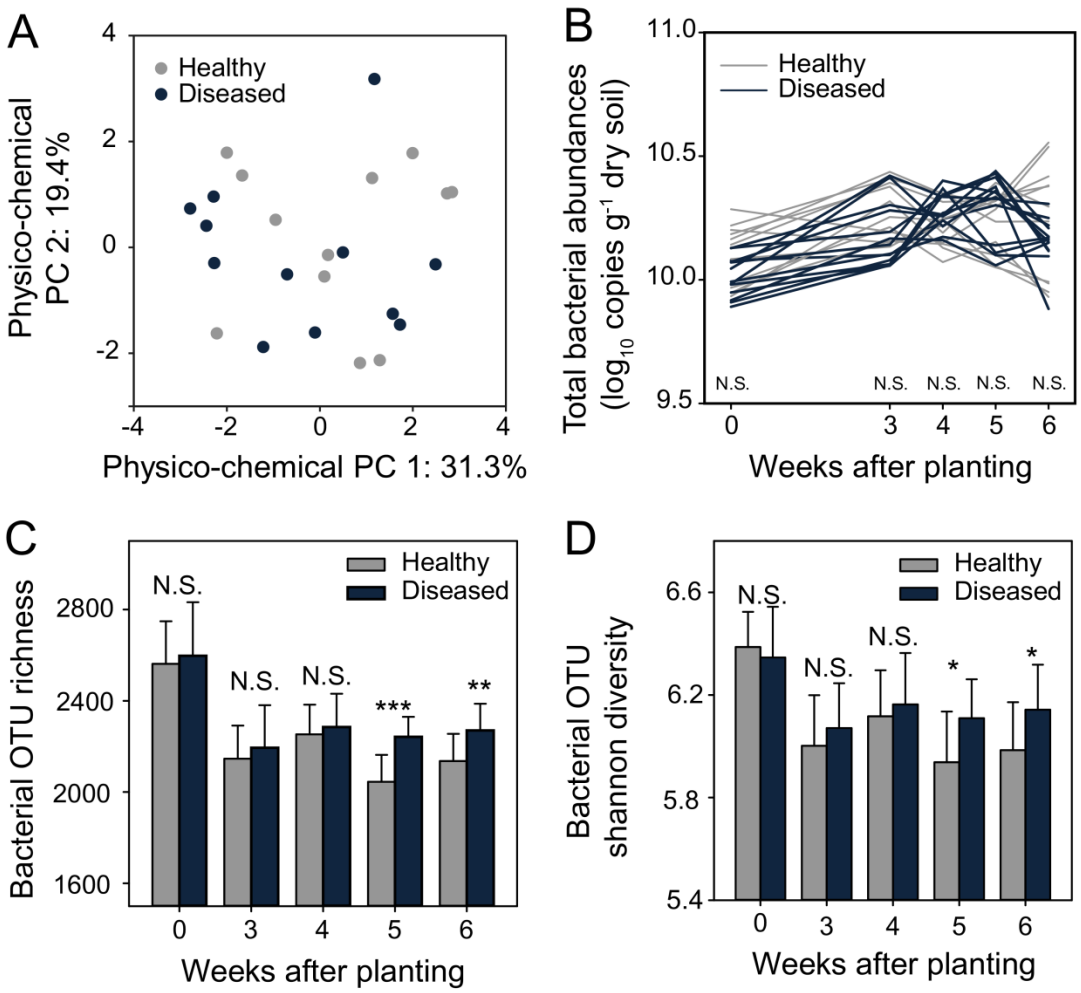


**Fig. S2. Differences in the physicochemical soil properties, total bacterial abundances, and bacterial diversity between healthy and diseased plants during the field experiment.** (**A**) Principal component analysis (PCA) of initial soil physiochemical properties. (**B**) Dynamics of total bacterial population densities in the microbiomes associated with healthy and diseased plants. (**C**) Differences in bacterial OTU richness in microbiomes associated with healthy and diseased plants. (**D**) Differences in bacterial Shannon diversity in microbiomes associated with healthy and diseased plants. In all panels, N.S. denotes non-significant difference, while * and *** indicate differences at $p < 0.05$ and 0.001 levels, respectively.

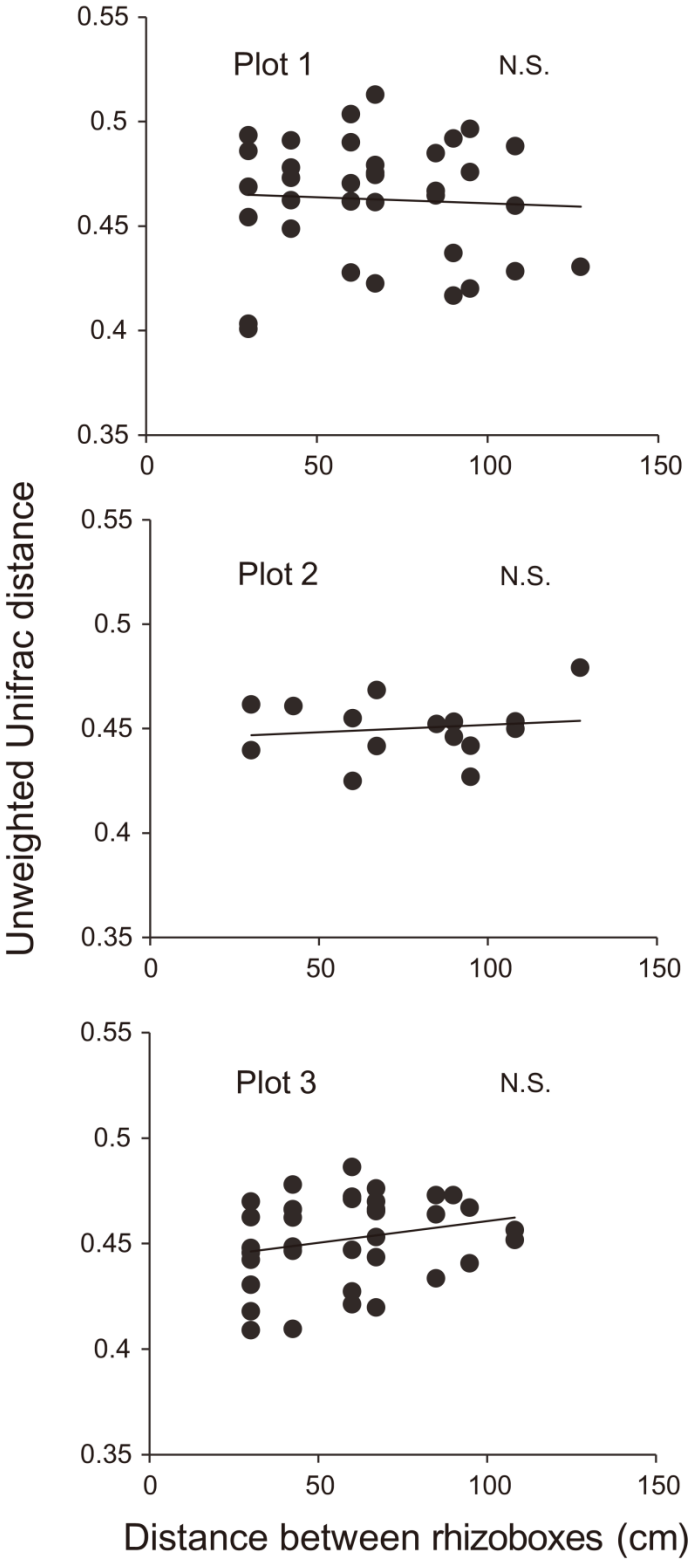


**Fig. S3. Relationships between physical distance and bacterial phylogenetic distance (unweighted UniFrac distance) between rhizoboxes within three replicated plots.**

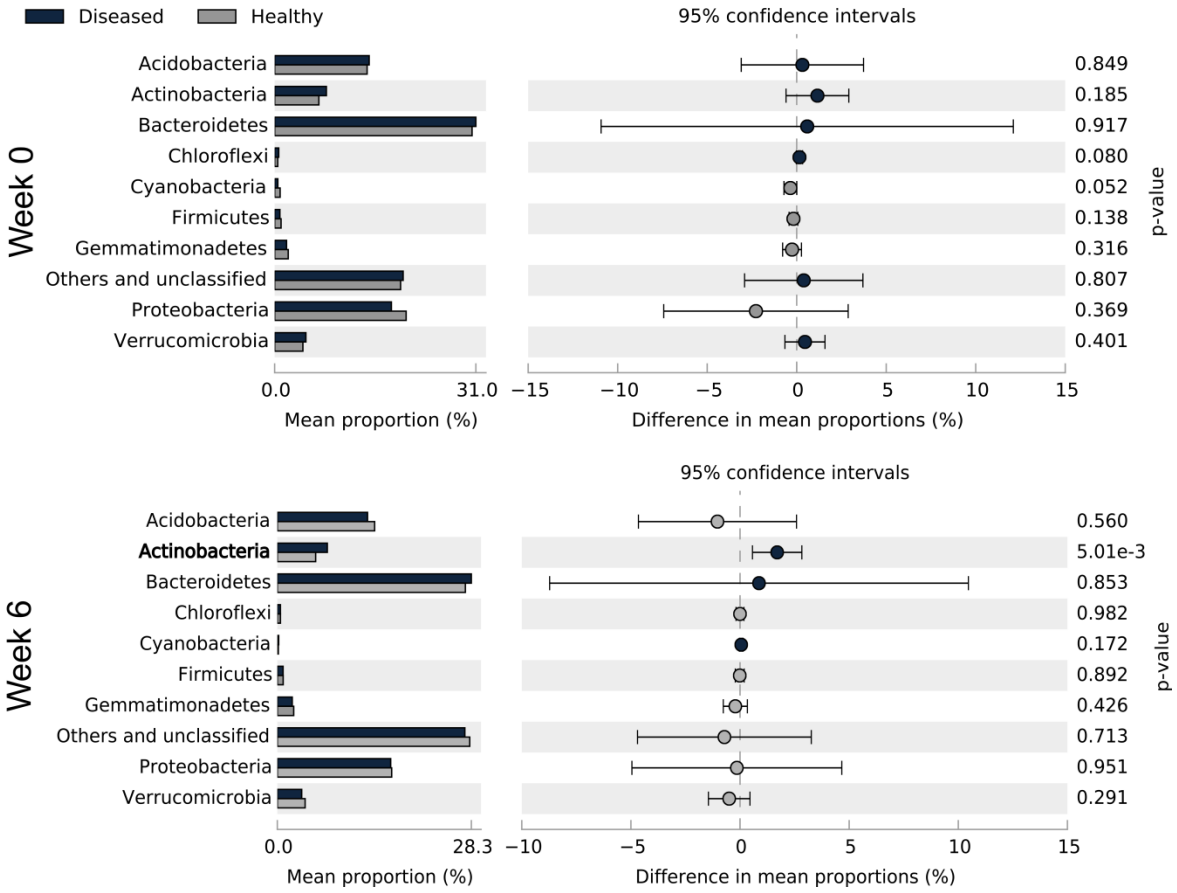


**Fig. S4. Differences in the abundances of bacterial phyla in the initial soils (week 0) that later became associated with healthy and diseased plants (week 6).** P-values were calculated using Student's t test ($p < 0.05$) and significantly associated phyla are highlighted in bold.

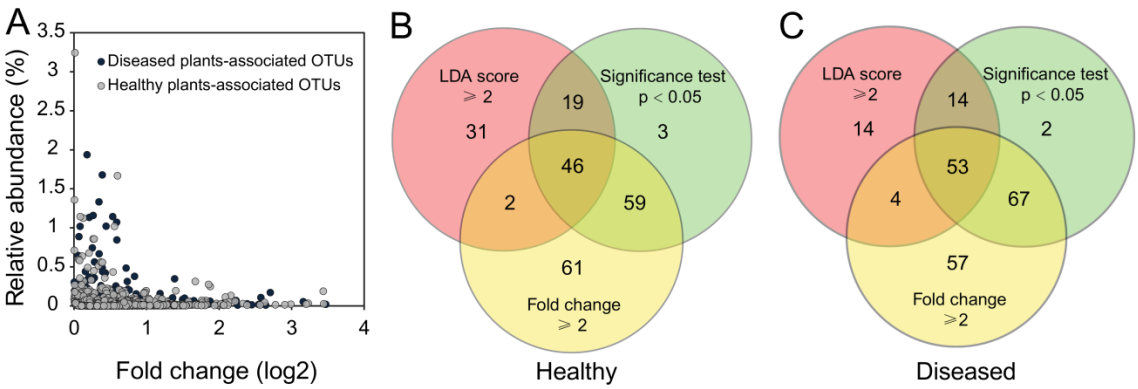


**Fig. S5. Rare OTUs discriminate the initial soil microbiomes that later become associated with healthy and diseased plants. (A)** Bacterial OTUs with low overall relative abundances discriminate initial soil microbiomes of future healthy and diseased plants. **(B-C)** Selection criteria for the most discriminating OTUs in initially healthy **(B)** and diseased **(C)** soils; Discriminating OTUs were identified based on three screening criteria: linear discriminant analysis (LDA) score $\geqslant$ 2; fold change $\geqslant$ 2 and significance test $p < 0.05$.

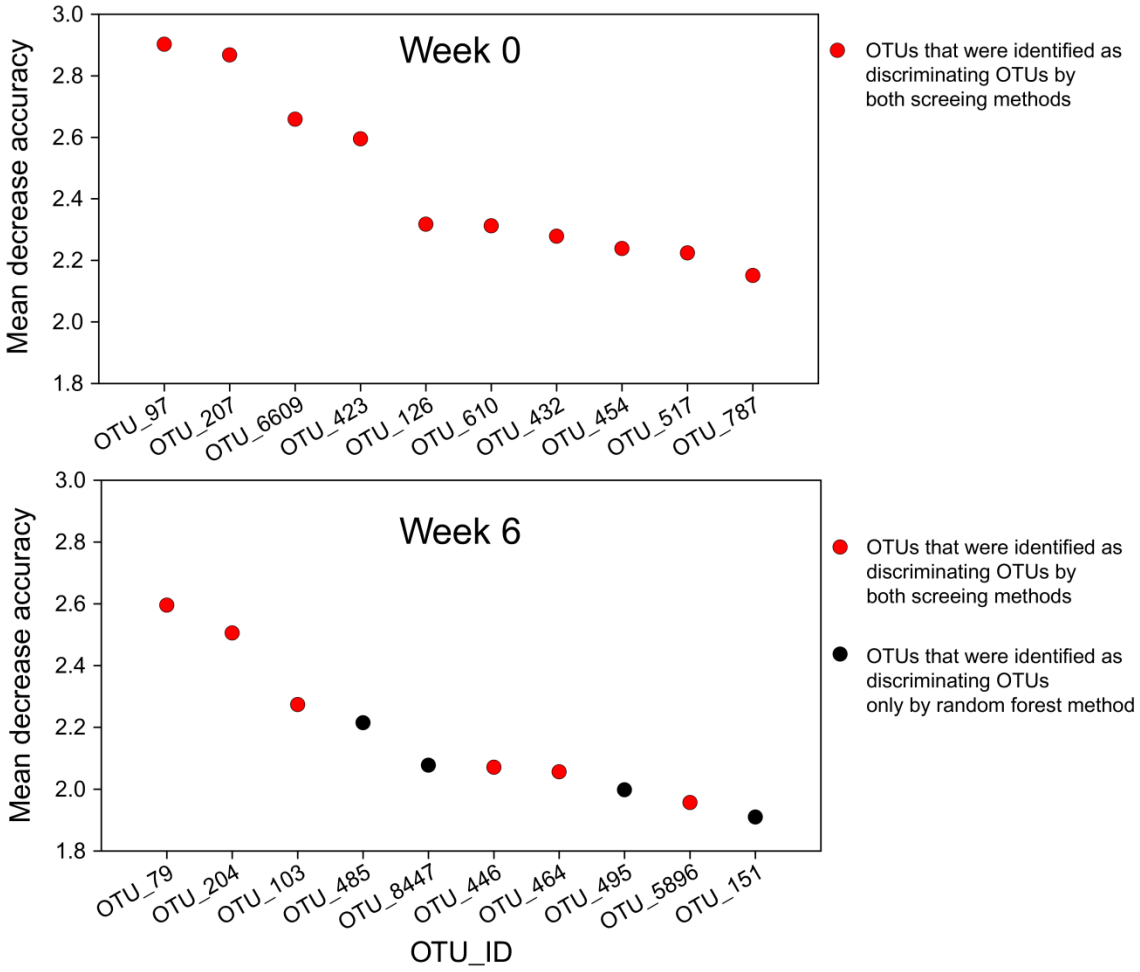


**Fig. S6. Ten best discriminant OTUs linked to future plant disease outcomes based on random forest analysis.** In both panels, red symbols denote for OTUs that were identified as discriminating OTUs by both our three screening criteria and random forest approaches, while black symbols denote for OTUs that were identified as discriminating OTUs only by random forest method. High mean decrease accuracy values denote the importance of predictor OTUs based on random forest analysis.

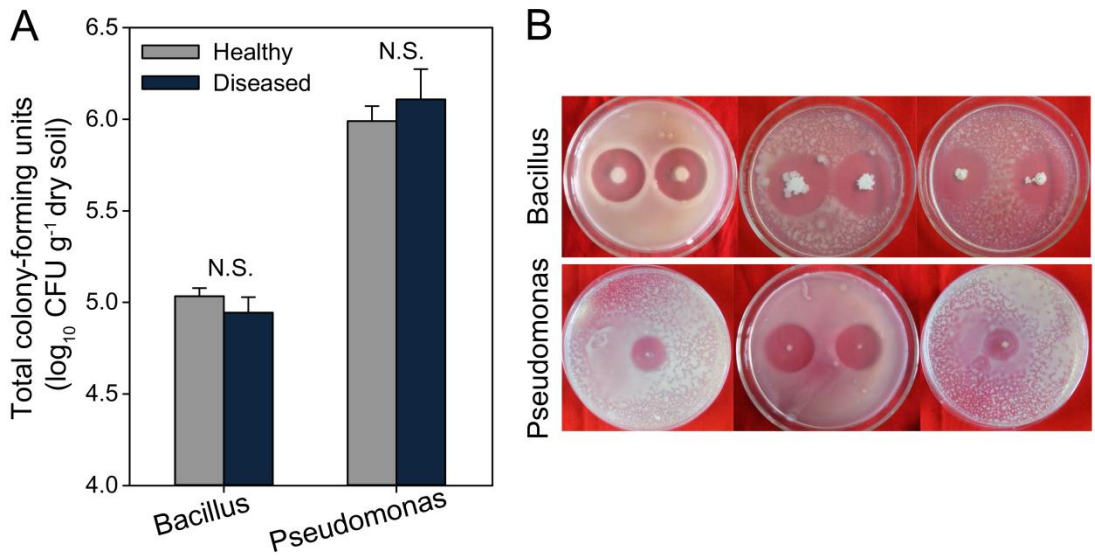


**Fig. S7. The total abundance of *Bacillus* and *Pseudomonas* bacteria and their ability to inhibit the growth of *Ralstonia solanacearum*.** The total *Bacillus* and *Pseudomonas* bacterial abundances isolated from initial soils associated with healthy and diseased plants (A, Mean ± SD, N = 3) and representative pictures of antagonistic effects of spotted (duplicates per plates) *Bacillus* and *Pseudomonas* strains on a lawn of *R. solanacearum* pathogen (B, Photo credit: Yian Gu, Nanjing Agricultural University). Bacteria were isolated using two semi-selective mediums: V8 for generic members of *Bacillus* and CFC for *Pseudomonas*. The N.S. denotes for non-significant difference.

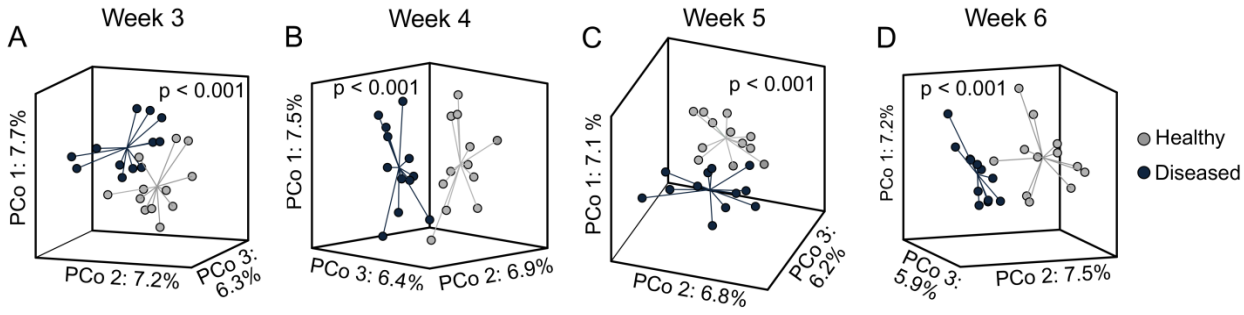


**Fig. S8. Differences in bacterial community composition associated with healthy and diseased plants persisted throughout the field experiment.** Distinct soil bacterial community compositions were associated with healthy and diseased plants at 3 **(A)**, 4 **(B)**, 5 **(C)** and 6 **(D)** weeks after planting of tomato seedlings to the field ($p < 0.001$, AMOVA on unweighted UniFrac). In all panels, individual points are connected by half-lines radiated from the centroid.

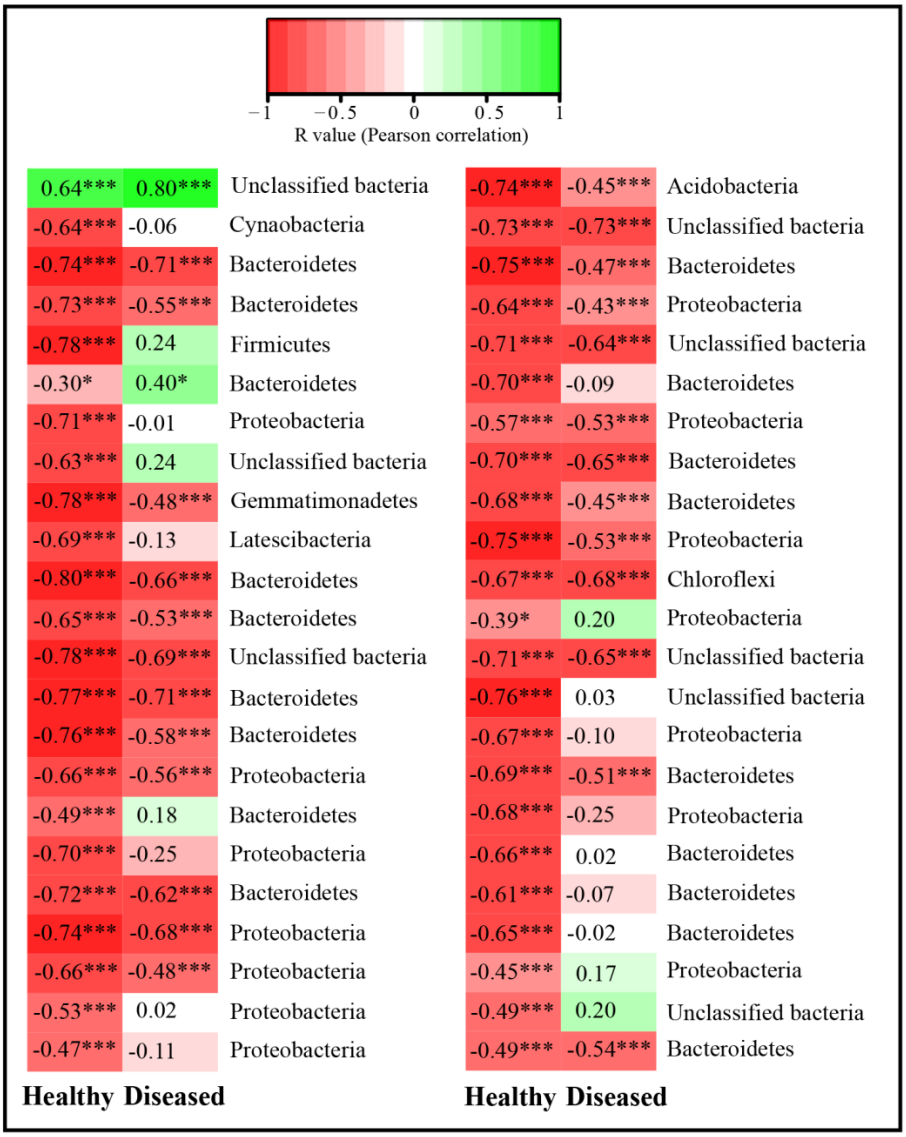


**Fig. S9. Temporal changes in discriminating rare OTUs observed in the initial microbiomes associated with healthy and diseased plants.** Most healthy plant-associated OTUs declined, while a large proportion of the diseased plant-associated OTUs increased during the tomato growth season. Table shows the Pearson correlation coefficients between time and the relative abundance of rare OTUs associated with healthy ("Healthy" column) and diseased ("Diseased" column) plants. Red color denote for negative correlations (OTUs that decreased in time) and green for positive

correlations (OTUs that increased in time); * and *** indicate significances at $p < 0.05$ and 0.001 levels, respectively.

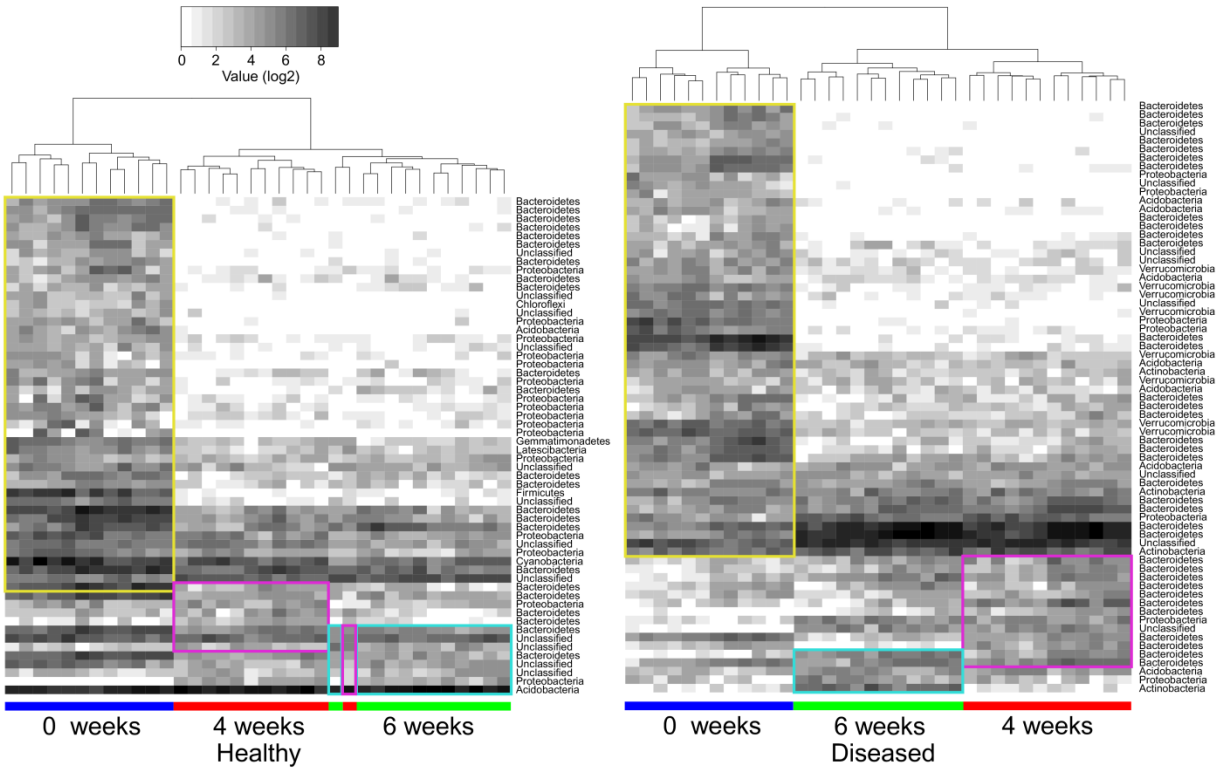


**Fig. S10. Heatmaps showing the dynamics of discriminating rare OTUs associated with healthy and diseased plants during the field experiment.** Screened OTUs enriched in soils associated with healthy (left panel) and diseased (right panel) plants at 0, 4, and 6 weeks after planting are highlighted with colored boxes.

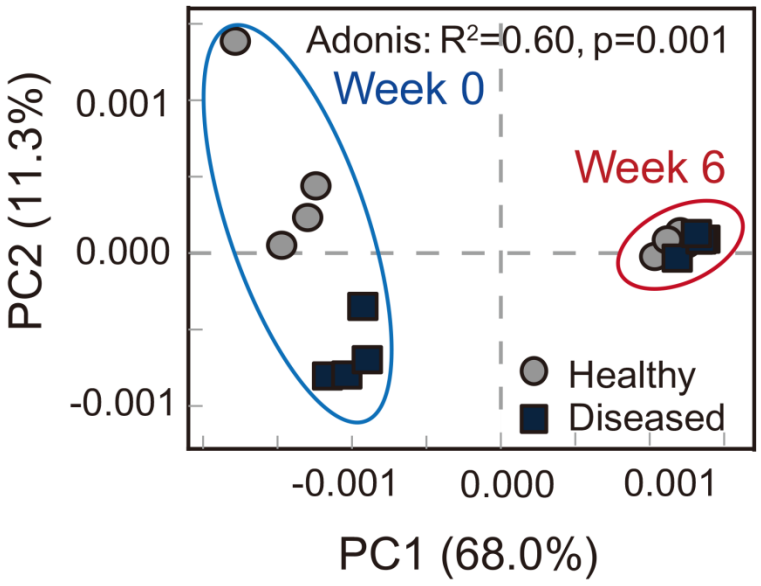


**Fig. S11. PCoA of Bray-Curtis distances of bacterial functional gene profiles in the beginning (week 0) and at the end of the field experiment (week 6).** Bacterial functional gene profiles were more different in the beginning compared to the end of the experiment. All Principal Coordinate Analyses (PCoA) were based on a Bray-Curtis dissimilarity index. The compositional differences in functional genes was analyzed using analysis of variance (Adonis) from R's vegan package.

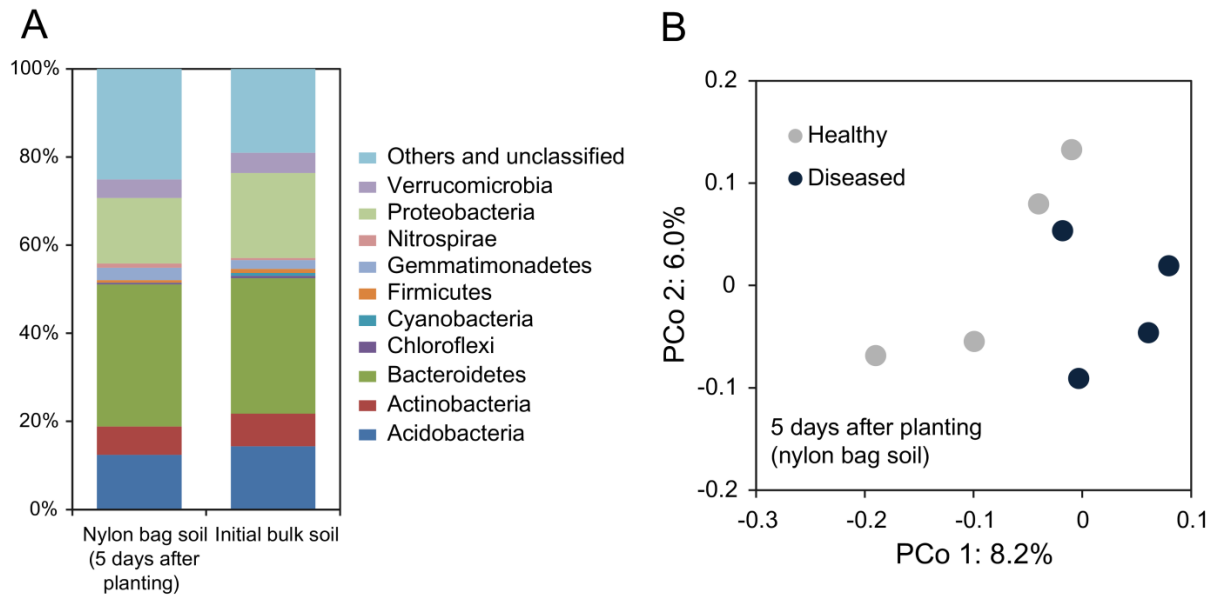


**Fig. S12. Comparison of bacterial community between initial bulk soil and 5-day old nylon bag samples.** Comparison of relative abundances of different bacterial phyla between initial bulk soil and 5-day old nylon bag samples (A). Principal coordinate analysis comparing differences (unweighted Unifrac distance) in bacterial community composition of 5-day old nylon bag soil samples, which were later associated with healthy and diseased plants (B).

**Table S1. Physicochemical properties of initial soils that later became associated with healthy and diseased plants.** Results show Mean ± SD. DOC: dissolved organic carbon, DON: dissolved organic nitrogen; $NH_4^+$-N and $NO_3^-$-N denote ammonium and nitrate nitrogen pools, respectively; AP, TC and TN denote available phosphate, total carbon and total nitrogen respectively. EC: electrical conductivity.

| Soil physico-chemical property | Healthy plant | Diseased plant | *P* value (t-test) |
|---|---|---|---|
| DOC (mg/kg) | 201.24 ± 50.82 | 170.6 ± 41.37 | 0.12 |
| DON (mg/kg) | 214.84 ± 40.43 | 208.86 ± 26.10 | 0.67 |
| $NH^{4+}$-N (mg/kg) | 24.31 ± 1.70 | 23.48 ± 1.64 | 0.24 |
| $NO_3^-$-N (mg/kg) | 237.32 ± 12.46 | 235.61 ± 7.39 | 0.69 |
| AP (mg/kg) | 140.89 ± 4.85 | 140.65 ± 5.23 | 0.76 |
| TN (%) | 0.63 ± 0.04 | 0.64 ± 0.03 | 0.48 |
| TC (%) | 1.97 ± 0.04 | 1.97 ± 0.08 | 0.92 |
| CN ratio | 3.15 ± 0.19 | 3.10 ± 0.22 | 0.52 |
| pH | 5.44 ± 0.10 | 5.4 ± 0.09 | 0.32 |
| EC (μs/cm) | 252.89 ± 62.33 | 238.77 ± 49.37 | 0.55 |

**Table S2. Topological properties of networks associated with healthy and diseased plant microbiomes at weeks 0 and 6.**

| Community | Number of nodes | Number of edges | Average connectivity | Modularity | Average path length | Average clustering coefficient |
|---|---|---|---|---|---|---|
| Healthy-week 0 | 511 | 1213 | 4.75 | 0.73 | 9.91 | 0.22 |
| Diseased-week 0 | 268 | 613 | 4.58 | 0.59 | 5.12 | 0.28 |
| Healthy-week 6 | 453 | 1277 | 5.64 | 0.71 | 7.49 | 0.31 |
| Diseased-week 6 | 391 | 1031 | 5.27 | 0.68 | 5.49 | 0.29 |